Clinical Neurophysiology 124 (2013) 770–778

Contents lists available at SciVerse ScienceDirect

Clinical Neurophysiology

journal homepage: www.elsevier.com/locate/clinph

Ocular vestibular evoked myogenic potentials induced by air-conducted sound in patients with acute brainstem lesions

Sun-Young Oh [a,b,*], Ji Soo Kim [c], Jong-Min Lee [d], Byoung-Soo Shin [a,b], Seung-Bae Hwang [b,e], Ki-Chang Kwak [d], Chanmi Kim [d], Seul-Ki Jeong [a,b], Tae-Woo Kim [a,b]

[a] Department of Neurology, Chonbuk National University School of Medicine, Jeonju, South Korea
[b] Research Institute of Clinical Medicine of Chonbuk National University-Chonbuk National University Hospital, Jeonju, South Korea
[c] Department of Neurology, Seoul National University Bundang Hospital, Seongnam, South Korea
[d] Department of Biomedical Engineering, Hanyang University, Seoul, South Korea
[e] Department Radiology, Chonbuk National University School of Medicine, Jeonju, South Korea

See Editorial, pages 640–641

ARTICLE INFO

Article history:
Available online 31 October 2012

Keywords:
Vestibular evoked myogenic potential (VEMP)
Ocular VEMPs (oVEMPs)
Air-conducted sound (ACS)
Otolith
Brainstem
Internuclear ophthalmoplegia (INO)
Medial longitudinal fasciculus (MLF)
Crossed ventral tegmental tract (CVTT)
Oculomotor nucleus

HIGHLIGHTS

- More than half of the patients with brainstem lesions showed abnormal air-conducted oVEMPs.
- The main lesion locations responsible for abnormal oVEMPs were the upper medial medulla, and the dorsomedial tegmentum of the pons and midbrain.
- Areas of the medial longitudinal fasciculus, the crossed ventral tegmental tracts and the oculomotor nucleus may carry the otolith-ocular signals required for oVEMP formation.

ABSTRACT

Objective: The ocular vestibular-evoked myogenic potential (oVEMP), a recently documented otolith-ocular reflex, is considered to reflect the central projections of the primary otolithic afferent fibers to the oculomotor nuclei. The aim of our study is to define air-conducted sound oVEMP abnormality in patients with acute brainstem lesions and to determine the brainstem structures involved in the generation of oVEMPs.
Methods: In response to air-conducted tone burst sounds (ACS), oVEMP was measured in 52 patients with acute brainstem lesions. Individualized brainstem lesions were analyzed by means of MRI-based voxel-wise lesion-behavior mapping, and the probabilistic lesion maps were constructed.
Results: More than half ($n = 28$, 53.8%) of the patients with acute brainstem lesions showed abnormal oVEMP in response to ACS. The majority of patients with abnormal oVEMPs had lesions in the dorsomedial brainstem that contains the medial longitudinal fasciculus (MLF), the crossed ventral tegmental tract (CVTT), and the oculomotor nuclei and nerves.
Conclusion: MLF, CVTT, and the oculomotor nuclei and nerves appear to be responsible for otolith-ocular responses in the brainstem.
Significance: Complemented to cervical VEMP for the uncrossed otolith-spinal function, oVEMP to ACS may be applied to evaluate the crossed otolith-ocular function in central vestibulopathies.

1. Introduction

Vestibular-evoked myogenic potentials (VEMPs) are now widely used to assess the otolith function. Cervical VEMP (cVEMP) is a manifestation of the vestibulocollic reflex and involves measuring the electromyographic (EMG) activity in the tonically-activated sternocleidomastoid (SCM) muscles (Chiappa, 1997; Colebatch and Rothwell, 1993; Colebatch et al., 1994; Curthoys,

* Corresponding author. Address: Department of Neurology, Chonbuk National University Hospital, Research Institute of Clinical Medicine, Chonbuk National University, 20 Geonji-ro, Deokjin-gu, Jeonju-city, Chonbuk 561-712, South Korea. Tel.: +82 63 250 1590; fax: +82 63 251 9363.
E-mail address: ohsun@jbnu.ac.kr (S.-Y. Oh).

1388-2457/$36.00
http://dx.doi.org/10.1016/j.clinph.2012.09.026

2012; Rosengren et al., 2010; Suzuki et al., 1969; Welgampola and Colebatch, 2001, 2005). VEMPs can also be recorded from the extraocular muscles using the surface electrodes placed over the inferior oblique and inferior rectus muscles, and termed ocular VEMP (oVEMP) (Chihara et al., 2007; Iwasaki et al., 2007, 2008; Rosengren et al., 2010; Shin et al., 2012; Suzuki et al., 1969; Todd et al., 2007; Welgampola et al., 2008). In contrary to cVEMP which is an uncrossed inhibitory vestibulospinal response, oVEMP reflects a crossed excitatory vestibulo (otolith)-ocular reflex (VOR) (Iwasaki et al., 2007, 2008, 2009; Todd et al., 2008). The VOR is mediated by a three-neuron link that consists of the vestibular receptors, the secondary neurons in the vestibular nuclei, and the ocular muscle motoneurons (Leigh and Zee, 2006). A major pathway carrying these signals is the medial longitudinal fasciculus (MLF). Also, other ascending pathways which convey the otolith signals from the vestibular nuclei to the upper brainstem and thalamus have been reported (Leigh and Zee, 2006; Graf and Ezure, 1986; Büttner-Ennever, 1992; Uchino et al., 1981; Zhu et al., 2011). However, the pathways by which otolith signals reach the ocular motor neurons for oVEMP remains unclear (Büttner-Ennever, 1999). There have been only a few studies on oVEMP in patients with brainstem lesions (Rosengren and Colebatch, 2011). Furthermore, the studies did not pursue a correlation between the lesion locations and normality of oVEMP. Therefore, in this study, we first aimed to clarify how often air-conducted oVEMP is abnormal in patients with acute brainstem lesions. Second, by comparing the involved brainstem regions between the groups of patients with normal and abnormal air-conducted oVEMPs, we attempted to determine the brainstem structures responsible for abnormal air-conducted oVEMPs and to find out the anatomic pathways in the brainstem by which the otolith signals reach the ocular motor neurons.

2. Methods

2.1. Patients

From March to December 2010, 52 patients (age range = 50–82, mean age ± SD = 63.8 ± 11.5, 32 men) with acute brainstem lesions of <1 month from symptom onset were enrolled in this study. The lesions were documented with MRI in all patients. Patients with concomitant lesions outside the brainstem, previous history of vertigo, dizziness or imbalance, or patients who have profound hearing loss before the event were excluded. Any patients with previous hearing impairment >20 dB or air-bone gap on pure tone audiometry were not included even though we did not perform tympanometry or stapedial reflex in all the patients. We also excluded the patients who were unable to cooperate by maintaining upward gaze during the test.

Patients also underwent detailed history taking, and general neurological and neuro-otological evaluation. The mean time from the disease onset to MRI was 3.6 ± 2.3 days (1 ∼ 14, median = 3) and to the oVEMP study was 4.9 ± 4.1 days (1 ∼ 18, median = 3). And the intervals from the oVEMP exam to MRI study were ranged 0 ∼ 13 days (mean ± SD = 3.2 ± 3.6) (Table 1). Patients were divided into normal and abnormal groups according to the results of oVEMPs. There were no differences in the interval from symptom onset to the studies of oVEMP and MRIs, and in other clinical variables between the groups (Table 1). This study was approved by the Institutional Review Board of Chonbuk National University Medical School.

2.2. Ocular VEMPs recording

For the recording of oVEMPs, we used air-conducted tone bursts. After the patients were laid supine with his/her head supported on a pillow, an active electrode was attached to the infraorbital ridge 1 cm below the center of each lower eyelid and a reference electrode was placed about 2 cm below the active electrode (Iwasaki et al., 2008, 2007; Rosengren et al., 2005; Todd et al., 2007). The ground electrode was attached to the forehead. During the testing, patients were instructed to keep staring at a small fixed point approximately 25° above at a distance of approximately 60 cm from the eyes (Shin et al., 2012). Stimuli were generated by customized software (Cadwell Laboratories, Kennewick, WA, USA). Using an insert earphone, sinusoidal AC tone bursts were delivered unilaterally with a negative polarity at 1000 Hz, 5 ms at an intensity of 100 dB nHL. Each stimulus consisted of a two-cycle rise and fall and one-cycle plateau. These stimuli were repeated at 5 Hz for 100 trials. Each ear was stimulated separately and oVEMP responses were obtained only from the eye contralateral to the stimulated ear. The signals were amplified by differential amplifiers, band-pass filtered (10–2000 Hz), and were sampled at 10 kHz from 2 ms before the stimulus onset to 50 ms afterwards. And then, the unrectified signals from 100 trials were averaged. The negative potentials detected through the active electrode were displayed as upward deflections. The amplitude of n10 was defined by the peak-to-peak difference of levels from the negative peak to the following positive peak. The abnormality of n10 amplitude was determined by asymmetry ratio (AR) that was calculated using the following formula: AR = (larger response–smaller response)/(larger response + smaller response) × 100. Since the AR of oVEMP amplitude was 14.4 ± 10.9% in normal controls (Shin et al., 2012), the oVEMP amplitude was defined as decreased in the smaller side when the AR was more than 40%. Also, oVEMP response was defined delayed when the n10 latency was >13.0 ms (normal range = 9.4 ± 1.8 ms).

Table 1
Characteristics of the patients with abnormal oVEMPs and normal oVEMPs.

Variables	Abnormal oVEMPs (n = 28, 53.8%)	Normal oVEMPs (n = 24, 46.1%)	p value*
Mean age ± SD (range)	65.8 (50 ∼ 82, 9.9 years)	61.5 (53 ∼ 82, 12.9 years)	0.18
Sex (M:F)	M:F = 17:11	M:F = 15:9	0.73
oVEMP from onset (days), mean (range, SD)	4.6 (1 ∼ 14, 3.9 days)	5.1 (2 ∼ 14, 4.3 days)	0.64
MRI from onset (days), mean (range, SD)	3.4 (1 ∼ 9, 1.8 days)	3.7 (1 ∼ 14, 2.8 days)	0.58
Interval between oVEMP and MRI (days), mean (range, SD)	2.4 (0 ∼ 12, 3.1 days)	4.2 (0 ∼ 13, 3.9 days)	0.07
Lesion volume, mean (mm^3, SD)	693.6 (1035)	607.7 (851)	0.23
95% confidence interval of the mean	256.5 ∼ 1130.7	263.8 ∼ 951.6	
INO (involving the MLF)	11	0	<0.01

SD = standard deviation; oVEMP = ocular vestibular evoked myogenic potentials; OTR = ocular tilt reaction; INO = internuclear ophthalmoplegia; MLF = medial longitudinal fasciculus.
* t-test or ANOVA.

Table 2
Clinical and demographic data of the 52 patients with brainstem lesions who presented normal and abnormal ocular VEMPs.

Lesion	Pt./age/sex	Site	Symptoms and signs	Lesion location	oVEMP[c]	
					Contralesional ear stimulation[a]	Ipsilesional ear stimulation[b]
Midbrain	1/69/M	Lt	3rd CN palsy (Lt), OTR, dizziness	Tegmentum	Absent	nl
	2/60/M	Lt	INO (Lt), OTR, hemiparesis (Rt), dizziness	Tegmentum (3rd CN)	Absent	nl
	3/69/F	Lt	INO (Lt), upgaze palsy, seesaw nystagmus, tremor	Tegmentum	Absent	nl
	4/81/M	Rt	Hemitremor, mild hemiparesis	Base (red nucleus)	Delayed	nl
	5/76/M	Lt	Dizziness, hemi-parkinsonism (Rt)	Paramedian tegmentum	nl	nl
Pons	6/75/F	Lt	INO (Lt), OTR	Tegmentum (MLF)	Absent	nl
	7/76/F	Lt	INO (Lt)	Tegmentum (MLF)	Absent	nl
	8/82/F	Lt	INO (Lt)	Tegmentum (MLF)	Absent	nl
	9/51/F	Rt	INO (Rt)	Tegmentum (MLF)	Absent	nl
	10/62/M	Rt	INO (Rt)	Tegmentum (MLF)	Absent	nl
	11/56/F	B	Bilateral INO, NMO	Bilateral tegmentum	Absent	Absent
	12/49/M	Lt	One and a half syndrome	Tegmentum	Absent	nl
	13/72/M	Lt	One and a half syndrome (Lt)	Tegmentum	Delayed	nl
	14/80/F	Lt	Dysarthria	Tegmentum	Delayed	nl
	15/55/M	Lt	AICA infarction, hearing loss (Lt)	Lateral inferior pontine	nl	Absent
	16/60/M	Rt	AICA infarction, hearing loss (Rt)	Lateral inferior pontine	nl	Absent
	17/69/M	Rt	Hemiparesis (Lt)	Medial midpontine	nl	Absent
	18/72/F	Lt	Dysarthria	Medial midpontine	nl	Absent
	19/75/M	Lt	Hemiparesis (Rt), dysarthria	Medial midpontine	nl	Absent
	20/67/M	Rt	Facial palsy (Rt), dysarthria	Lateral midpontine	nl	Absent
	21/33/M	Rt	Hemisensory loss (Lt), MS	Lateral midpontine	nl	nl
	22/73/M	Rt	Hemisensory loss (Lt), dysphagia	Base	nl	nl
	23/82/M	Lt	Hemiparesis (Rt), dysarthria	Medial midpontine	nl	nl
	24/55/M	Rt	Hemiparesis (Lt), dysarthria	Base	nl	nl
	25/65/F	Rt	Hemiparesis (Lt)	Medial midpontine	nl	nl
	26/76/M	Rt	Hemiparesis (Lt)	Medial midpontine	nl	nl
	27/73/F	Lt	Hemiparesis (Rt), dysarthria	Medial midpontine	nl	nl
	28/72/M	Rt	Dysarthria	Medial midpontine	nl	nl
	29/64/F	Rt	Hemiparesis (Lt), facial palsy(Lt)	Medial midpontine, base	nl	nl
	30/67/M	Lt	Hemiparesis (Rt), dysarthria	Medial midpontine	nl	nl
	31/53/F	Lt	Hemiparesis (Rt)	Medial midpontine	nl	nl
	32/71/M	Rt	Sensory change (Lt)	Tegmentum	nl	nl
	33/75/M	Rt	Diplopia, dysarthria	Medial midpontine	nl	nl
Medullar	34/60/M	Rt	Diplopia, upbeat nys., MMI	Medial medulla	Absent	nl
	35/63/M	Lt	Diplopia, upbeat nys., dizziness, MMI	Medial medulla	Absent	nl
	36/62/M	Rt	Hemiparesis (Lt), left-beat nys., MMI	Medial medulla	Absent	nl
	37/75/F	Rt	Hemiparesis (Lt), dizziness, MMI	Medial medulla	nl	Absent
	38/77/F	Lt	Dizziness, right-beat nyst., GEN, MMI	Medial medulla	Absent	Absent
	39/61/M	Rt	Vertigo, dysphagia	Lateral medulla	Absent	nl
	40/43/F	Lt	Ptosis, dysphagia, dysarthria, sensory loss (Rt)	Lateral medulla	Delayed	nl
	41/57/M	Lt	Vertigo, headache, metastasis	Lateral medulla	nl	Absent
	42/71/M	Lt	Vertigo, oscillopsia, ataxia	Lateral medulla	Absent	Absent
	43/41/M	Lt	Dysarthria, vertigo, numbness	Lateral medulla	nl	nl
	44/55/M	Lt	Dysphagia, horner (Rt), sensory loss (Rt)	Lateral medulla	nl	nl
	45/60/F	Rt	Facial palsy, horner (Rt), dysarthria	Lateral medulla	nl	nl
	46/56/F	Rt	Ptosis, dysphagia, dysarthria, nystagmus	Lateral medulla	nl	nl
	47/68/F	Rt	Hemiparesis, nystagmus, vertigo, ataxia	Lateral medulla	nl	nl
	48/55/M	Lt	Dysphagia, horner (Lt), GEN, dysphagia	Lateral medulla	nl	nl
	49/58/M	Rt	Sensory loss (Lt), dysarthria, ataxia	Lateral medulla	nl	nl
	50/56/F	Rt	Horner (Rt), ataxia	Lateral medulla	nl	nl

51/47/F	Lt	Sensory loss (Lt), horner (Lt)	Lateral medulla	nl		nl
52/41/M	B	Hemiparesis (Rt), upbeat nys., medullary hemorrhage	Central medulla	nl		nl

AICA = anterior inferior cerebellar artery syndrome; B = bilateral; GEN = gaze-evoked nystagmus; HL = concurrent hearing loss; INO = internuclear ophthalmoplegia; OTR = ocular tilt reaction; Lt = left; MMI = medial medullary infarction; NA = no tested; NMO = neuromyelitis optica; nl = normal; oVEMP = ocular vestibular evoked myogenic potential; Rt = right; VA dissection = vertebral artery dissection.

[a] Contralesional ear stimulation and ipsilesional eye recording.

[b] Ipsilesional ear stimulation and contralesional eye recording.

[c] Compare to normal data (Shin et al., 2012).

2.3. MR and Image processing

MRI data were captured on a 3.0 T scanner (Verio, Siemens, Erlangen, Germany) using our standard imaging protocol including diffusion-weighted imaging (DWI) and fluid-attenuated inversion recovery (FLAIR) sequences. A statistical parametric mapping, SPM8 (FIL Methods Group, UK, http://www.fil.ion.ucl.ac.uk/spm), was used for image registration. MATLAB (Mathworkd Inc., USA) software package was adopted for the implementation of the statistical parametric mapping for neuroimaging analysis. This software has been designed for the analysis of brain imaging data sequences. The lesions that appeared on DWI or FLAIR image data were co-registered into the International Consortium for Brain Mapping (ICBM) 152 template using a 12-parameter affine transformation, and the resulting transformation was used to transfer the lesion map from their native space to the standard space. Lesions were traced onto the templates by a neurologist (Kim) who was blinded to the clinical information in order to prevent the knowledge of the test results from biasing the drawing of lesion boundaries. We combined the results of all patients by flipping the drawn images of the lesions in the patients with left-sided lesion. To identify the anatomic structures that were specifically damaged in the patients with abnormal oVEMPs, we subtracted the superimposed lesion images of the normal oVEMP patients from the overlapped images in the abnormal oVEMPs group. The lesion map was semi-automatically segmented by the Otsu algorithm (Otsu, 1979). We estimated the fraction of each lesion map within each voxel to obtain the probabilistic lesion maps in the standard space. The algorithm for estimating the probabilistic lesion maps was implemented by MATLAB.

2.4. Statistical analysis

Data from all patients were divided into normal and abnormal oVEMP responses to the ACS, allowing the results from all patients to be averaged together, regardless of the side of the lesions. Comparative analysis of the results of lesion volume and acuteness of the studies between the normal and abnormal patient groups was done using the Student's *t*-tests, and clinical findings between the groups were compared using the chi-square and analysis of variance (ANOVA). All statistical procedures were performed using Statistical Package for Social Sciences (SPSS) statistical software version 14.

3. Results

3.1. Air-conducted sound oVEMP findings

Among the 52 patients, 48 had ischemic stroke involving the midbrain ($n = 5$), pons ($n = 26$), or medulla ($n = 17$). The remaining four patients had multiple sclerosis ($n = 2$) involving the dorsomedial pons and pontocerebellar peduncle, medullary hemorrhage ($n = 1$), and metastatic lesion in the lower medulla ($n = 1$) (Table 2). Twenty-seven (28/52, 53.8%) patients showed abnormal oVEMPs (Tables 1 and 2).

Of the five patients with acute midbrain lesions, four (4/5, 80%) showed abnormal air-conducted oVEMPs during contralesional ear stimulation, but preserved responses during ipsilesional ear stimulation. Three of them showed absent air-conducted oVEMPs on the contralesional ear stimulation and these patients had the 3rd cranial nerve palsy and unilateral internuclear ophthalmoplegia (INO) with contralesional SVV tilt and ocular tilt reaction (OTR) (Fig. 1A). One patient with Weber syndrome with hemiparkinsonism (Pt. 4) showed delayed n10 during contralesional ear stimulation (Table 2).

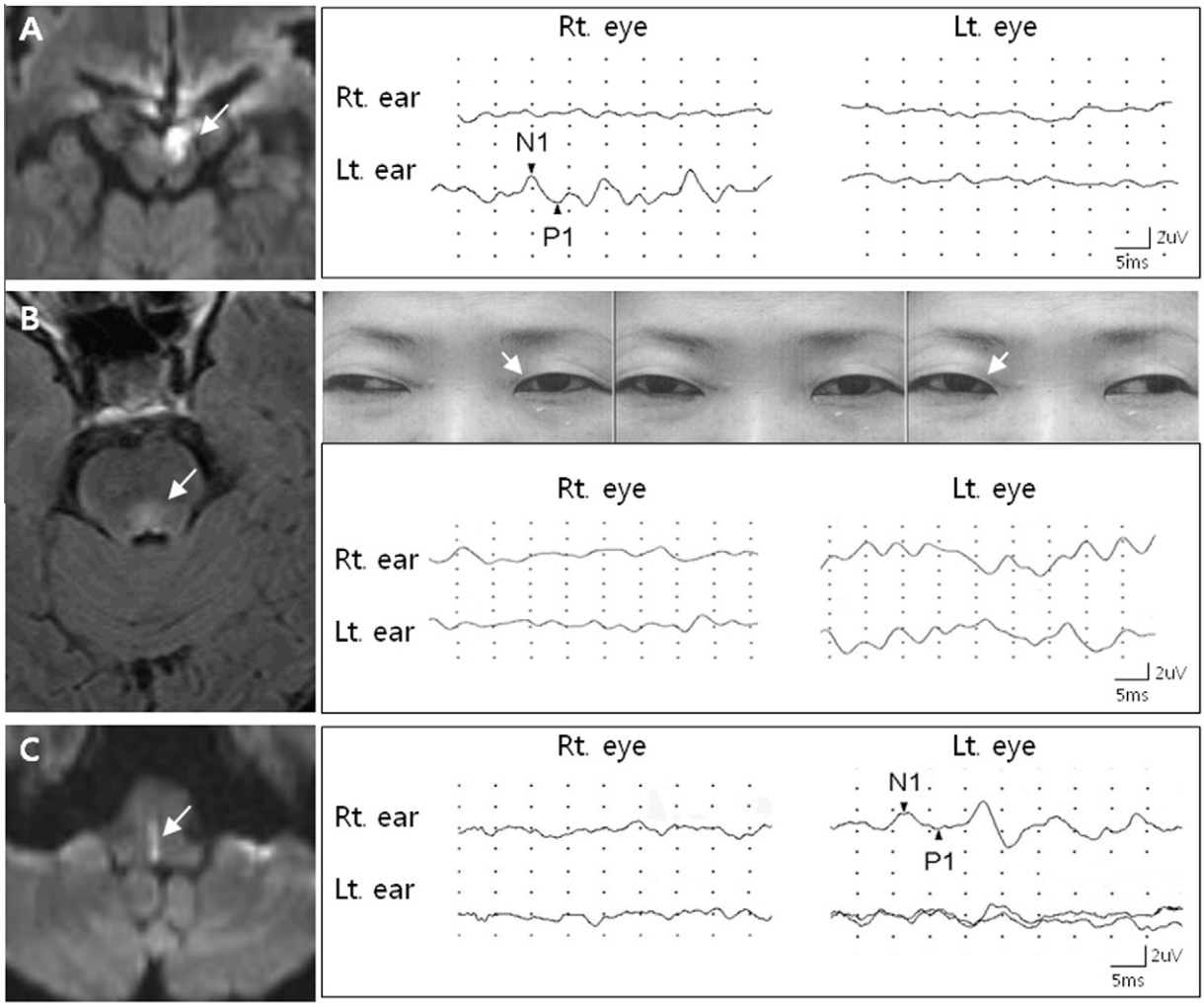

Fig. 1. Ocular vestibular-evoked myogenic potentials (oVEMPs) recorded from 3 representative patients with brainstem lesion at each level in response to stimulation at 1000 Hz, 5 ms tone bursts. (A) A 60-year-old man (Pt. 2, Table 2) with left third cranial nerve palsy and upgaze limitation shows absent oVEMPs from the ipsilesional left eye during the contralesional right ear stimulation. (B) A 56-year-old woman (Pt. 11, Table 2) with bilateral internuclear ophthalmoplegia from neuromyelitis optica involving bilateral dorsomedial pontine tegmentum shows bilateral absence of oVEMP. (C) A 60-year-old man (Pt. 34, Table 2) with right medial medullary infarction shows no formation of oVEMPs from the ipsilesional right eye during contralesional left ear stimulation.

Of the 28 patients with acute pontine lesions, 16 (57.1%) showed abnormal oVEMP to ACS. Among them, five patients (Pt. 6 ~ 10) had unilateral (ipsilesional) INO and exhibited no wave formation of air-conducted oVEMP during the contralesional ear stimulation. During ipsilesional ear stimulation, however, normal negative peak responses were recorded. One neuromyelitis optica (NMO) patient (Pt. 11) with bilateral INO showed absence of air-conducted oVEMP bilaterally (Fig. 1B). Two patients with one-and-a-half syndrome showed absence (Pt. 12) or delayed (Pt. 13) formation of air-conducted oVEMPs during contralesional ear stimulation. Patients with anterior inferior cerebellar artery (AICA) infarction (Pt. 15 and 16) and ipsilesional hearing loss showed no

Table 3
Abnormalities of oVEMPs in patients with brainstem lesions.

		Abnormal oVEMP			Normal oVEMP
		Contralesional ear[a]	Ipsilesional ear[b]	Bilateral	
Midbrain ($N = 5$)	Absent Delayed	$N = 3$ $N = 1$			$N = 1$
Pons ($N = 28$)	Absent Delayed	$N = 6$ $N = 2$	$N = 6$ or 4[c]	$N = 1$	$N = 13$
Medulla	Absent Delayed	$N = 4$ $N = 1$	$N = 2$	$N = 2$	$N = 10$
Total ($N = 52$)		$N = 17$ (60.7%)	$N = 8$ (28.5%) or 4 (15.4%)[c]	$N = 3$ (10.7%)	$N = 24$

[a] Contralesional ear stimulation and ipsilesional eye recording.
[b] Ipsilesional ear stimulation and contralesional eye recording.
[c] After excluding 2 patients with ipsilateral hearing loss due to AICA infarction.

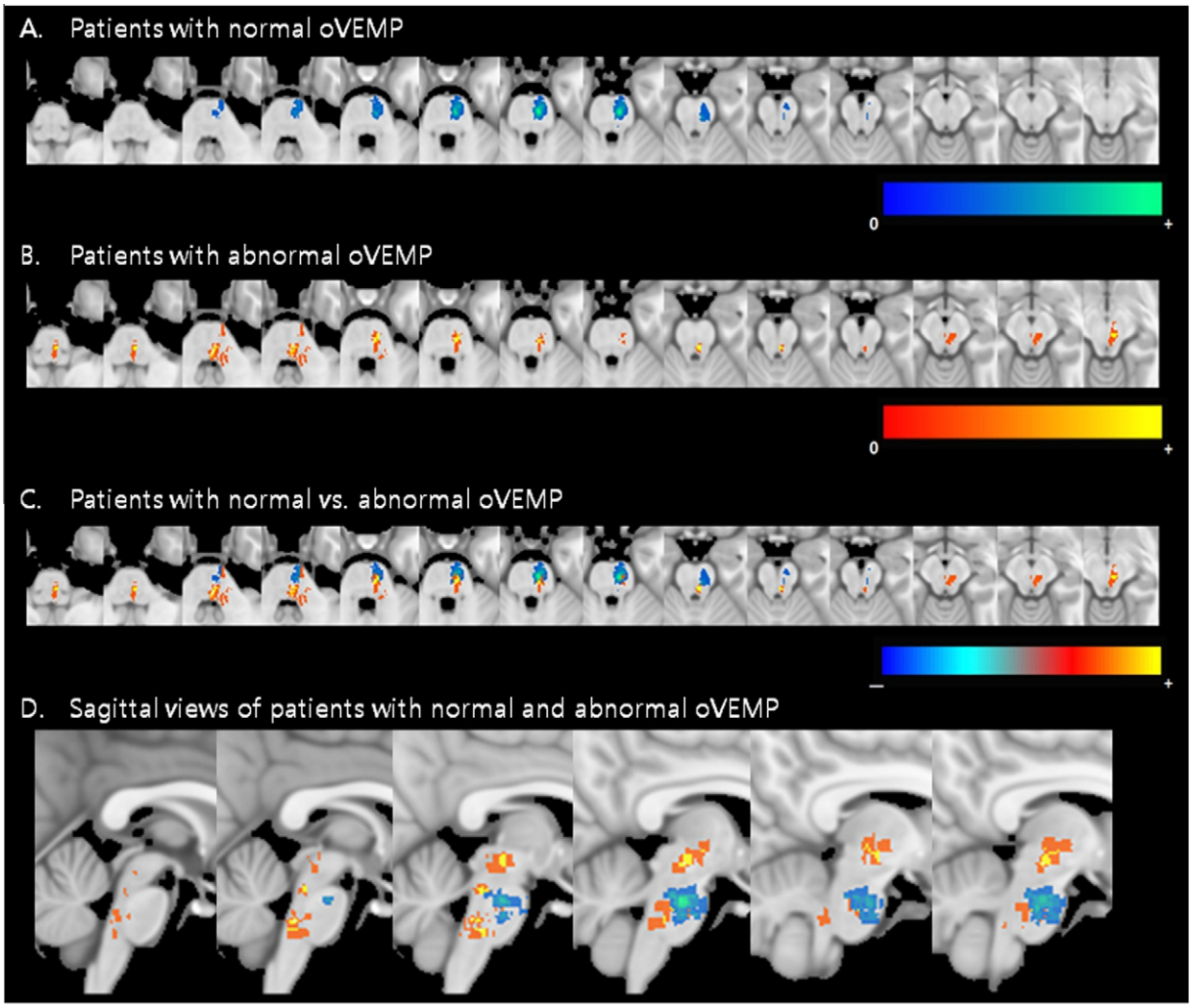

Fig. 2. Probabilistic lesion maps. (A) Lesion map of 24 patients with normal oVEMPs. The number of overlapping lesions is illustrated by the color codes which vary from blue to light green as the frequency increases. (B) The lesion profiles of patients with unilaterally abnormal oVEMP. Right-sided lesions are flipped to the left. (C) The difference-map of the subtracted superimposed lesions between the normal and abnormal oVEMP groups. The lesions associated with normal VEMPs are visualized in blue colors and the lesions associated with abnormal VEMPs are visualized in red colors. The legend of color codes is shown in the lower right corner. (D) The sagittal diagram labeling the lesion areas in the brainstem with each color coding in patients with normal and abnormal oVEMPs. Note that the lesions associated with normal oVEMP are located in the ventral areas including the basis pontis while the lesions with abnormal oVEMP are located in the mediodorsal areas in the brainstem. (For interpretation of the references to color in this figure legend, the reader is referred to the web version of this article.)

formation of air-conducted oVEMPs during ipsilesional ear stimulation. Absence of oVEMP in patients with AICA infarction was due to concurrent hearing loss and these two patients' image data were not included in analysis. Remaining patients with lesions involving the medial anterior midpontine area showed mostly normal air-conducted oVEMPs (Table 2).

Of the 19 patients with medullary lesions, all five with upper medial medullary lesions showed abnormal air-conducted oVEMPs. Three of them (Pt. 34 ~ 36) exhibited absence of air-conducted oVEMP only during contralesional ear stimulation (Fig. 1C) while two had absent formation only during ipsilesional ear stimulation (Pt. 38) or no wave formation bilaterally (Pt. 37). Patients with lateral medullary lesion showed abnormal results less frequently than patients with the medial medullary lesions (4/14, 28.5%) (Table 2).

In our series, all unilateral INO patients ($n = 7$) showed absent oVEMP during contralesional ear stimulation and bilateral INO patient ($n = 1$, Pt. 11) did not generate oVEMP bilaterally (Fig. 1B). Two patients with one-and-a-half syndrome also exhibited absent (Pt. 12) or delayed (Pt. 13) responses of oVEMP only during contralesional ear stimulation (Table 2). Most patients with abnormal air-conducted oVEMP showed absence of responses (24/28, 85.7%) rather than delayed responses (4/28, 14.3%), which is consistent with the ischemic pathology in the majority of our patients (Table 3).

3.2. Correlation between lesions and abnormal air-conducted sound oVEMP

From the lesion mapping analyses, we found that the brainstem lesions responsible for abnormal air-conducted oVEMPs lie in the paramedian dorsal aspects of the brainstem from the upper medulla oblongata to the midbrain, which include the medial longitudinal fasciculus (MLF), middle cerebellar peduncle, the crossed ventral tegmental tract (CVTT) and the oculomotor nucleus and nerve in the midbrain (Fig. 2). In contrast, air-conducted oVEMPs were mostly spared in the lesions involving the anteromedial part of the brainstem.

4. Discussion

In contrast to cVEMP that reflects descending uncrossed sacculocollic pathway in the lower brainstem (Colebatch et al., 1994;

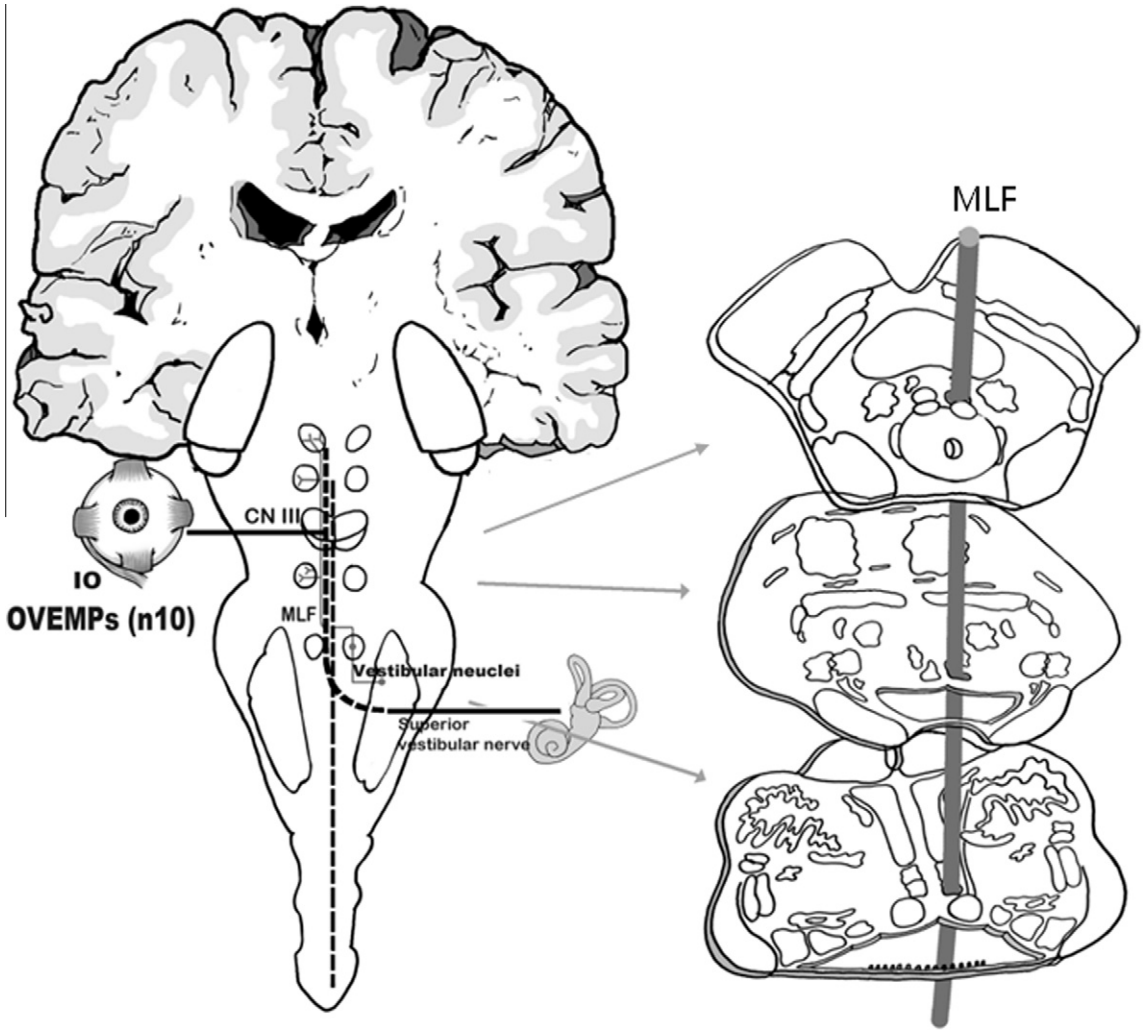

Fig. 3. The medial longitudinal fasciculus (MLF) may be the main pathway of crossed otolith-ocular reflex responsible for ocular vestibular-evoked myogenic potential. CN III = third cranial nerve.

Kim et al., 2010; Rosengren et al., 2010; Welgampola and Colebatch, 2001, 2005), the oVEMP may be mediated by ascending connection to the oculomotor nuclei and probably a manifestation of crossed otolith-ocular reflex pathways (Curthoys, 1987; Iwasaki et al., 2007, 2008; Rosengren and Colebatch, 2011; Rosengren et al., 2010; Shin et al., 2012; Todd et al., 2007; Welgampola et al., 2008). In normal subjects, the oVEMP responses were larger in the eye contralateral to the stimulated ear than in the ipsilateral eye (Iwasaki et al., 2009; Shin et al., 2012). Furthermore, patients with unilateral vestibular loss showed that the oVEMP was invariably reduced or absent in the contralesional eye (Iwasaki et al., 2007, 2008; Shin et al., 2012). The anatomic and functional organization of brainstem otolithic pathway for oVEMP, however, remains unclear (Büttner-Ennever, 1999; Uchino et al., 1996; Suzuki et al., 1969; Zhu et al., 2011). Primary afferents from the otoliths terminate mainly in the lateral, inferior and caudal superior vestibular nuclei (Uchino et al., 2005). The otolithic efferents from the vestibular nuclei descend via reticulo- and vestibulospinal pathways in the spinal cord to influence neck motoneurons and ascend to the oculomotor neurons. In this study, we attempted to determine the abnormality of oVEMP to ACS in the brainstem lesions, and to define the neural structures responsible for transfer of crossed otolithic signals to the oculomotor nuclei and formation of oVEMP. Our study revealed that more than half (53.8%) of the patients with acute brainstem lesions had abnormal oVEMPs to ACS. The main lesion locations responsible for abnormal air-conducted oVEMPs were the upper medial medulla, and the dorsomedial tegmentum of the pons and midbrain. These areas correspond to MLF, CVTT, and the oculomotor nucleus and nerves. These findings suggest that these structures carry the otolith-ocular signals required for air-conducted oVEMP formation.

Vestibular information is conveyed from the vestibular nuclei to the oculomotor and trochlear nuclei and the interstitial nucleus of Cajal and the rostral interstitial nucleus of the medial longitudinal fasciculus through several pathways including MLF, the ascending tract of Deiters (ATD), and CVTT (Maciewicz et al., 1982; Lang et al., 1979; Brandt and Dieterich, 1993). The major pathway of vestibular projections arising from the semicircular canals and otolithic organs is MLF which is located in the dorsal midline of the brainstem and mostly crossed (Zwergal et al., 2008) (Fig. 3). In our series, 10 of the 28 patients (35.7%) with abnormal oVEMP had uni-/bilateral INO or one-and-a-half syndrome due to lesions involving MLF. All these patients with MLF involving lesions showed abnormal oVEMP results, which is similar to the data reported recently (Rosengren and Colebatch, 2011). In addition to MLF, ATD and CVTT have been suggested as possible routes for the ipsilateral and contralateral otolithic projections in the brainstem, respectively (Maciewicz et al., 1982; Lang et al., 1979). ATD lies lateral to MLF and is known to project ipsilaterally to the oculomotor nuclei (Maciewicz et al., 1982). However, ATD may hardly be a struc-

ture responsible for abnormal oVEMP since the otolith-ocular projection involved in the generation of oVEMP is known to be primarily crossed (Iwasaki et al., 2007, 2008; Shin et al., 2012). Another vestibulo-oculomotor fibers that cross in a broadly scattered band is CVTT which include the fibers toward the ocular motoneurons that innervates the inferior oblique and superior rectus (Uchino et al., 1994). Bilateral lesions of CVTT have been associated with upbeat nystagmus (Pierrot-Deseilligny and Milea. 2005).

The amplitude and latency of VEMPs also depend on age (Murofushi et al., 2001; Welgampola and Colebatch, 2001; Basta et al., 2007), and bilaterally absent or delayed VEMPs may be found in the elderly (Tseng et al., 2010). It is also known that oVEMP thresholds are higher than cVEMP thresholds at all frequencies and the absence rate of oVEMP in response to 1000 Hz sound is around 5% (Park et al., 2010). Delays in evoked potentials are typical of demyelination, and VEMPs have been reported to be delayed in multiple sclerosis (Chiappa, 1997). Demyelination is expected to affect the tracts, mostly in the root entry zone, as opposed to the nuclei. In contrast, ischemic or hemorrhagic stroke may involve either the tracts or nuclei and can give rise to delayed or absent responses. In our study, most patients with abnormal oVEMP showed absence of responses (24/28, 85.7%) and only 4 (4/28, 14.3%) exhibited delayed responses from the infarction.

Our study has limitations by defining the ischemic lesion extent based on DWI findings. Even though DWI and fluid attenuated inversion recovery (FLAIR) MRIs are highly sensitive in detecting acute brainstem lesions, DWI is subject to motion artifacts (Lin et al., 2007) and may fail to reveal the hyperacute ischemic lesions (Wang et al., 1999). False-negative MRI can occur during the acute period of ischemic stroke and the region may be variable depending on the evolution state of ischemia. However, most of our patients were stable during both pre- and post-MRI periods without a marked evolution of the symptoms and signs. Even though we excluded the patients with air-bone gap on audiometry, the possibility of middle ear pathology could not be completely eliminated without tympanometry and stapedial reflexes.

Although the vestibular afferents respond to both air- (Curthoys and Vulovic 2011; Murofushi et al., 2001; Murofushi and Curthoys 1997) and bone-conducted sounds (Curthoys et al., 2006; Curthoys and Vulovic 2011), the present study recorded oVEMP in response to air-conducted tone burst sounds only. Since we did not measure oVEMPs induced by bone-conducted vibration, the normality of oVEMP in response to bone-conducted vibration cannot be excluded in our patients. Recent oVEMP studies found that about 500 Hz is the optimal frequency to generate oVEMPs (Park et al., 2010; Donnellan et al., 2010). In this study, we used 1000 Hz frequencies of stimuli, which may have resulted in higher prevalence of abnormality. However, we believe that the effect would be minimal, if any, since we determined the abnormality by comparing the responses from both eyes.

In conclusion, our study revealed that more than half (53.8%) of the patients with acute brainstem lesions showed abnormal oVEMP in response to ACS. The abnormal oVEMPs were mostly associated with lesions in the dorsomedial tegmentum from the upper medulla oblongata to the midbrain where MLF, CVTT and the oculomotor nuclei and nerves locate (Figs. 2 and 3). These results support the hypothesis that oVEMP is mediated by these structures. Ocular VEMP to ACS is useful for examining the crossed otolith-ocular function in the central vestibulopathies, and is complementary to cVEMP that reflects uncrossed otolith-spinal function.

5. Disclosure

The authors report no conflicts of interest.

Acknowledgements

This work was supported by Research Institute of Clinical Medicine of Chonbuk National University-Chonbuk National University Hospital and by the Korea Science and Engineering Foundation (KOSEF) NLRL Program Grant funded by the Korean Government (MEST) (2011-0028333).

References

Basta D, Todt I, Ernst A. Characterization of age-related changes in vestibular evoked myogenic potentials. J Vestib Res 2007;17:93–8.
Brandt T, Dieterich M. Skew deviation with ocular torsion: a vestibular brainstem sign of topographic diagnostic value. Ann Neurol 1993;33:528–34.
Büttner-Ennever JA. Patterns of connectivity in the vestibular nucleia. Ann NY Acad Sci 1992;656:363–78.
Büttner-Ennever JA. A review of otolith pathways to brainstem and cerebellum. Ann NY Acad Sci 1999;871:51–64.
Chiappa KH. Evoked potentials in clinical medicine. Lippincott-Raven New York; 1997.
Chihara Y, Iwasaki S, Ushio M, Murofushi T. Vestibular-evoked extraocular potentials by air-conducted sound: another clinical test for vestibular function. Clin Neurophysiol 2007;118:2745–51.
Curthoys I. Eye movements produced by utricular and saccular stimulation. Aviat Space Environ Med 1987;58:192–7.
Curthoys IS, Kim J, McPhedran SK, Camp AJ. Bone conducted vibration selectively activates irregular primary otolithic vestibular neurons in the guinea pig. Exp Brain Res 2006;175:256–67.
Curthoys IS, Vulovic V. Vestibular primary afferent responses to sound and vibration in the guinea pig. Exp Brain Res 2011;210:347–52.
Curthoys IS. The interpretation of clinical tests of peripheral vestibular function. Laryngoscope 2012;122:1342–52.
Colebatch JG, Halmagyi GM, Skuse NF. Myogenic potentials generated by a click-evoked vestibulocollic reflex. J Neurol Neurosurg Psychiatry 1994;57:190–7.
Colebatch JG, Rothwell JC. Vestibular-evoked EMG responses in human neck muscles. J Physiol 1993;473:18.
Donnellan K, Wei W, Jeffcoat B, Mustain W, Xu Y, Eby T, Zhou W. Frequency tuning of bone conducted tone burst-evoked myogenic potential in extraocular muscles (BOVEMP) in normal human subjects. Laryngoscope 2010;120:2555–61.
Graf W, Ezure K. Morphology of vertical canal related second order vestibular neurons in the cat. Exp Brain Res 1986;63:35–48.
Iwasaki S, McGarvie L, Halmagyi G, Burgess A, Kim J, Colebatch J, et al. Head taps evoke a crossed vestibulo-ocular reflex. Neurology 2007;68:1227–9.
Iwasaki S, Smulders Y, Burgess A, McGarvie L, MacDougall H, Halmagyi G, et al. Ocular vestibular evoked myogenic potentials to bone conducted vibration of the midline forehead at Fz in healthy subjects. Clin Neurophysiol 2008;119:2135–47.
Iwasaki S, Chihara Y, Smulders YE, Burgess AM, Halmagyi GM, Curthoys IS, et al. The role of the superior vestibular nerve in generating ocular vestibular-evoked myogenic potentials to bone conducted vibration at Fz. Clin Neurophysiol 2009;120:588–93.
Kim S, Lee HS, Kim JS. Medial vestibulospinal tract lesions impair sacculo-collic reflexes. J Neurol 2010;257:825–32.
Lang W, Buttner-Ennever JA, Buttner U. Vestibular projections to the monkey thalamus: an autoradiographic study. Brain Res 1979;177:3–17.
Leigh RJ, Zee DS. The neurology of eye movements. 4th ed. New York: Oxford University Press; 2006.
Lin T, Sun H, Chen Z, You R, Zhong J. Numerical simulations of motion-insensitive diffusion imaging based on the distant dipolar field effects. Magn Reson Imaging 2007;25:1409–16.
Maciewicz R, Phipps BS, Bry J, Highstein SM. The vestibulothalamic pathway: contribution of the ascending tract of Deiters. Brain Res 1982;252:1–11.
Murofushi T, Curthoys IS. Physiological and anatomical study of click-sensitive primary vestibular afferents in the guinea pig. Acta Otolaryngol 1997;117:66–72.
Murofushi T, Shimizu K, Takegoshi H, Cheng PW. Diagnostic value of prolonged latencies in the vestibular evoked myogenic potential. Arch Otolaryngol Head Neck Surg 2001;127:1069–72.
Otsu N. A threshold selection method from gray-level histograms. IEEE Transactions on Systems, Man and Cybernetics 1979;9:62–6.
Park HJ, Lee IS, Shin JE, Lee YJ, Park MS. Frequency-tuning characteristics of cervical and ocular vestibular evoked myogenic potentials induced by air-conducted tone bursts. Clin Neurophysiol 2010;121:85–9.
Pierrot-Deseilligny C, Milea D. Vertical nystagmus: clinical facts and hypotheses. Brain 2005;128:1237–46.
Rosengren SM, McAngus Todd NP, Colebatch JG. Vestibular-evoked extra ocular potentials produced by stimulation with bone-conducted sound. Clin Neurophysiol 2005;116:1938–48.
Rosengren S, Welgampola M, Colebatch J. Vestibular evoked myogenic potentials: past, present and future. Clin Neurophysiol 2010;121:636–51.

Rosengren SM, Colebatch JG. Ocular vestibular evoked myogenic potentials are abnormal in internuclear ophthalmoplegia. Clin Neurophysiol 2011;122:1264–7.

Shin B-S, Oh S-Y, Kim JS, Kim T-W, Seo M-W, Lee H, et al. Cervical and ocular vestibular-evoked myogenic potentials in acute vestibular neuritis. Clin Neurophysiol 2012;123:369–75.

Suzuki JI, Tokumasu K, Goto K. Eye movements from single utricular nerve stimulation in the cat. Acta Otolaryngol 1969;68:350–62.

Tseng CL, Chou CH, Young YH. Aging effect on the ocular vestibular-evoked myogenic potentials. Otol Neurotol 2010;31:959–63.

Todd NP, Rosengren SM, Aw ST, Colebatch JG. Ocular vestibular evoked myogenic potentials (OVEMPs) produced by air- and bone-conducted sound. Clin Neurophysiol 2007;118:381–90.

Todd NP, Rosengren SM, Colebatch JG. Ocular vestibular evoked myogenic potentials (OVEMPs) produced by impulsive transmastoid accelerations. Clin Neurophysiol 2008;119:1638–51.

Uchino Y, Hirai N, Suzuki S, Watanabe S. Properties of secondary vestibular neurons fired by stimulation of ampullary nerve of the vertical, anterior or posterior, semicircular canals in the cat. Brain Res 1981;223:273–86.

Uchino Y, Sasaki M, Isu N, Hirai N, Imagawa M, Endo K, et al. Second-order vestibular neuron morphology of the extra-MLF anterior canal pathway in the cat. Exp Brain Res 1994;97:387–96.

Uchino Y, Sasaki M, Sato H, Imagawa M, Suwa H, Isu N. Utriculoocular reflex arc of the cat. J Neurophysiol 1996;76:1896–903.

Uchino Y, Sasaki M, Sato H, Bai R, Kawamoto E. Otolith and canal integration on single vestibular neurons in cats. Exp Brain Res 2005;164:271–85.

Wang PY, Barker PB, Wityk RJ, Ulug AM, van Zijl PC, Beauchamp Jr NJ. Diffusion-negative stroke: a report of two cases. Am J Neuroradiol 1999;20:1876–80.

Welgampola MS, Colebatch JG. Vestibulocollic reflexes: normal values and the effect of age. Clin Neurophysiol 2001;112:1971–9.

Welgampola MS, Colebatch JG. Characteristics and clinical applications of vestibular-evoked myogenic potentials. Neurology 2005;64:1682–8.

Welgampola MS, Myrie OA, Minor LB, Carey JP. Vestibular-evoked myogenic potential thresholds normalize on plugging superior canal dehiscence. Neurology 2008;70:464–72.

Zhu H, Tang X, Wei W, Mustain W, Xu Y, Zhou W. Click-evoked responses in vestibular afferents in rats. J Neurophysiol 2011;106:754–63.

Zwergal A, Cnyrim C, Arbusow V, Glaser M, Fesl G, Brandt T, et al. Unilateral INO is associated with ocular tilt reaction in pontomesencephalic lesions. Neurology 2008;71:590–3.